The Journal of Membrane Biology (2022) 255:1–12
https://doi.org/10.1007/s00232-021-00198-7

Metabolic Depletion of Sphingolipids Does Not Alter Cell Cycle Progression in Chinese Hamster Ovary Cells

Bhagyashree D. Rao[1] · Parijat Sarkar[1] · Amitabha Chattopadhyay[1]

Received: 6 July 2021 / Accepted: 2 August 2021 / Published online: 14 August 2021

Abstract

The cell cycle is a sequential multi-step process essential for growth and proliferation of cells comprising multicellular organisms. Although a number of proteins are known to modulate the cell cycle, the role of lipids in regulation of cell cycle is still emerging. In our previous work, we monitored the role of cholesterol in cell cycle progression in CHO-K1 cells. Since sphingolipids enjoy a functionally synergistic relationship with membrane cholesterol, in this work, we explored whether sphingolipids could modulate the eukaryotic cell cycle using CHO-K1 cells. Sphingolipids are essential components of eukaryotic cell membranes and are involved in a number of important cellular functions. To comprehensively monitor the role of sphingolipids on cell cycle progression, we carried out metabolic depletion of sphingolipids in CHO-K1 cells using inhibitors (fumonisin B_1, myriocin, and PDMP) that block specific steps of the sphingolipid biosynthetic pathway and examined their effect on individual cell cycle phases. Our results show that metabolic inhibitors led to significant reduction in specific sphingolipids, yet such inhibition in sphingolipid biosynthesis did not show any effect on cell cycle progression in CHO-K1 cells. We speculate that any role of sphingolipids on cell cycle progression could be context and cell-type dependent, and cancer cells could be a better choice for monitoring such regulation, since sphingolipids are differentially modulated in these cells.

Graphic Abstract

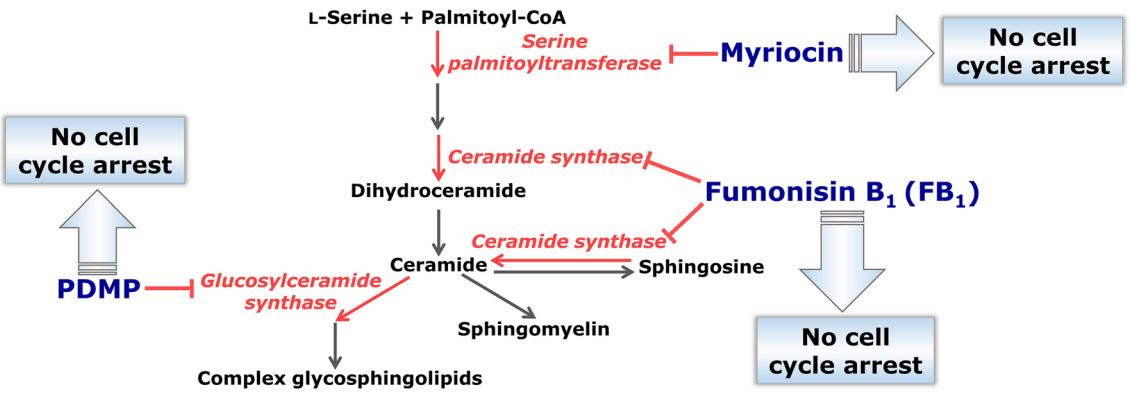

Keywords Sphingolipid depletion · Cell cycle · Fumonisin B_1 · Myriocin · PDMP

Introduction

Sphingolipids are essential, ubiquitous components of eukaryotic cell membranes and comprise ~ 10–20% of total membrane lipids (Holthuis et al. 2001). They play a crucial role in the regulation of diverse cellular processes such as

✉ Amitabha Chattopadhyay
amit@ccmb.res.in

[1] CSIR-Centre for Cellular and Molecular Biology, Uppal Road, Hyderabad 500 007, India

signaling, proliferation, and senescence, and are involved in the pathophysiology of neurological disorders (Zeidan and Hannun 2007; van Echten-Deckert and Walter 2012; Sonnino and Prinetti 2016; Hannun and Obeid 2018; Hussain et al. 2019). It has been proposed that sphingolipids along with cholesterol form ordered lipid domains, often referred as 'lipid rafts' which are laterally segregated from the bulk membrane (Simons and Ikonen 1997). These microdomains facilitate the interaction of signaling partners, thereby leading to efficient signal transduction in processes such as protein sorting and pathogen entry into cells (Simons and van Meer 1988; Simons and Toomre 2000; Ramstedt and Slotte 2006; Riethmüller et al. 2006; Klemm et al. 2009; Viswanathan et al. 2018). Importantly, sphingolipids have been shown to modulate the function of important membrane proteins such as G protein-coupled receptors (GPCRs) and ion channels (Sabbadini et al. 1999; Mahfoud et al. 2002; Fantini 2003; Fantini and Barrantes 2009; Dart 2010; Paila et al. 2010; Rosenhouse-Dantsker et al. 2012; Singh et al. 2012; Jafurulla and Chattopadhyay 2015; Jafurulla et al. 2017; Olsen and Færgeman 2017).

The abundance of sphingolipids in the plasma membrane is higher relative to intracellular membranes (Lange et al. 1989). Sphingolipid production and abundance has been shown to be tightly regulated by several metabolic enzymes, whose altered activity could lead to modulation in signaling processes, especially in cancer (Ogretmen 2018). The sphingolipid biosynthetic pathway (see Fig. 1) is initiated by the condensation of L-serine with palmitoyl-CoA, which is catalyzed by the enzyme serine palmitoyltransferase at the cytoplasmic face of the endoplasmic reticulum. This eventually leads to formation of sphinganine which acts as the building block of sphingolipids. Subsequently, ceramide is synthesized by acylation of sphinganine or sphingosine catalyzed by the enzyme ceramide synthase (*N*-acetyltransferase). Ceramide is then translocated from ER to the Golgi apparatus (Fukasawa et al. 1999; Baier and Barrantes 2007) and is either converted to sphingomyelin

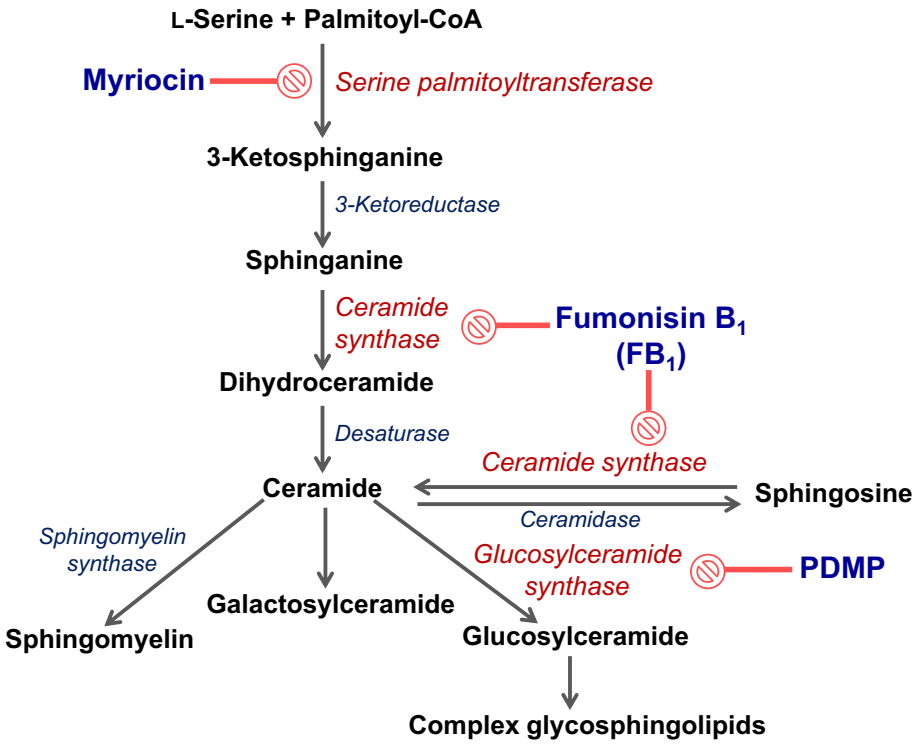

Fig. 1 Metabolic pathway for sphingolipid biosynthesis and commonly used inhibitors in various stages of the pathway. The role of sphingolipids in cellular processes has been explored using specific inhibitors that target enzymes catalyzing key steps in the biosynthetic pathway. Representative enzymes which could be targeted in the biosynthetic pathway and specific inhibitors that act on these enzymes are highlighted. The rate-limiting step in the de novo biosynthetic pathway of sphingolipids is catalyzed by the enzyme serine palmitoyltransferase in the endoplasmic reticulum. Subsequent reactions in the pathway lead to synthesis of ceramides, which are converted into complex sphingolipids (majorly in the Golgi), including glycosphingolipids and sphingomyelin. Myriocin is a fungal metabolite which acts as a competitive inhibitor of the rate-limiting enzyme serine palmitoyltransferase that leads to the synthesis of 3-ketosphinganine. Fumonisin B_1 (FB_1), a naturally occurring mycotoxin produced by several *Fusarium* species, is a competitive inhibitor of the enzyme ceramide synthase (*N*-acetyltransferase) which catalyzes the acylation of either sphinganine or sphingosine, thereby inhibiting the synthesis of ceramide and other complex sphingolipids. On the other hand, PDMP is a synthetic analog of ceramide and a competitive inhibitor of the enzyme glucosylceramide synthase which is the first enzyme in the biosynthesis of glycosphingolipids. See text for more details

by the enzyme sphingomyelin synthase on the luminal face of the Golgi, or to glucosylceramide by the enzyme glucosylceramide synthase, on the cytosolic surface of the Golgi apparatus. Further, glucosylceramide is converted to complex glycosphingolipids upon translocation into the Golgi lumen (van Meer and Lisman 2002). Sphingolipids exhibit enormous structural diversity in terms of different types of fatty acids (of varying chain length, extent of saturation, and hydroxylation) attached to the sphingoid base and the polar headgroups connected to ceramide (Fantini and Barrantes 2009; Jafurulla and Chattopadhyay 2015).

Cell cycle is an organized series of events which occurs continuously in living cells of multicellular organisms and results in multiplication of cells for growth as well as tissue repair (Schafer 1998; Harper and Brooks 2005). The eukaryotic cell cycle is comprised of four discrete phases which are the G1 (gap 1) phase, S (synthesis) phase, G2 (gap 2) phase, and M (mitosis) phase. The different phases of cell cycle in a population of cells can be distinguished depending on the alteration in cellular DNA content using flow cytometry (see Fig. 2). The transition from one phase of the cell cycle to the next is tightly regulated by several checkpoints at specific intervals in the cell cycle. The proper maintenance of these checkpoints is essential for cell survival, since it guarantees that a cell has satisfied all the necessary requirements for transitioning into successive cell cycle stages (Barnum and O'Connell 2014). An imbalance in the cell division process due to various mutations in the protein machinery that regulates the checkpoints in cell cycle leads to cancer.

A large number of proteins in the cytoplasm and nucleus are known to be involved in cell cycle regulation (Barnum and O'Connell 2014), whereas the role of membrane lipids in cell cycle regulation is not explored well. In this context, we previously utilized distal and proximal inhibitors of cholesterol biosynthetic pathway and showed that the requirement of cholesterol for G1 to S transition is absolute, and even immediate biosynthetic precursors of cholesterol, differing with cholesterol merely in a double bond, could not replace cholesterol for reversing the cell cycle arrest (Singh et al. 2013). In addition, we showed that cholesterol content is modulated across various stages of the cell cycle in a cell-type specific manner (Singh et al. 2013; Sarkar et al. 2020). However, the role of sphingolipids in cell cycle progression has not been explored in detail. Since sphingolipids enjoy a synergistic relationship with membrane cholesterol (Slotte and Bierman 1988; Slotte et al. 1990; García-Arribas et al. 2016; Róg et al. 2016; Slotte 2016), in this work, we explored whether sphingolipids could modulate the eukaryotic cell cycle. For this, we carried out metabolic depletion of sphingolipids in Chinese hamster ovary (CHO-K1) cells using inhibitors that act in specific steps of the sphingolipid biosynthesis pathway and monitored the effect on individual cell cycle phases.

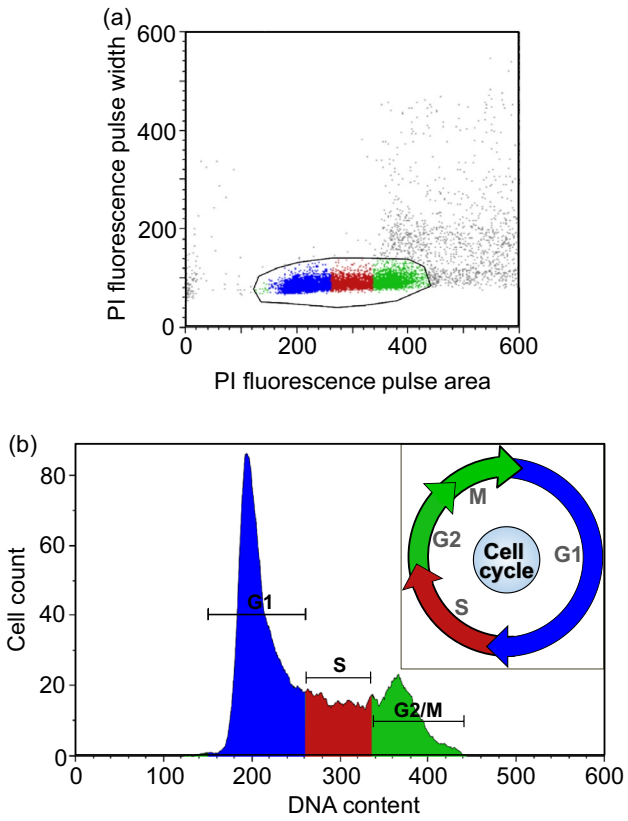

Fig. 2 Flow cytometric analysis of asynchronous CHO-K1 cells. **a** Pulse width analysis of CHO-K1 cells labeled with propidium iodide was performed to distinguish singlet cells from multiplet population of cells. **b** Representative flow cytometric profile of asynchronous CHO-K1 cells obtained after labeling with propidium iodide. The histogram represents cell distribution in G1 (blue), S (red), and G2/M (green) phases of the cell cycle. Inset shows a schematic representation of the cell cycle phases according to the time spent in each phase. See text and Materials and Methods for more details

Materials and Methods

Materials

3-(4,5-Dimethylthiazol-2-yl)-2,5-diphenyl-tetrazolium bromide (MTT), dimethyl sulfoxide (DMSO), EDTA, fumonisin B_1 (FB_1), gentamicin sulfate, myriocin, oleic acid-albumin complex, (±)-threo-1-phenyl-2-decanoylamino-3-morpholino-1-propanol (PDMP), penicillin, propidium iodide, sodium bicarbonate, streptomycin, and Tris were obtained from Sigma Chemical Co. (St. Louis, MO). RNase A was obtained from Calbiochem (San Diego, CA). Nutridoma-SP was from Roche Applied Science (Mannheim, Germany). Porcine brain sphingomyelin was purchased from Avanti Polar Lipids (Alabaster, AL) and neutral glycosphingolipid mixture was from Matreya LLC (State College, PA). DMEM/F-12 [Dulbecco's modified Eagle's medium/nutrient mixture F-12 (Ham) (1:1)] and fetal calf serum (FCS)

were from Invitrogen/Life Technologies (Grand Island, NY). Bicinchoninic acid (BCA) reagent for protein estimation was from Pierce (Rockford, IL). Precoated silica gel 60 thin layer chromatography plates were from Millipore (Bedford, MA). All other chemicals and solvents used were of the highest available purity. Water was purified through a Millipore (Bedford, MA) Milli-Q system and used throughout.

Cell Culture

CHO-K1 cells were maintained in DMEM/F-12 (1:1) medium supplemented with 2.4 g/l of sodium bicarbonate, 10% (v/v) FCS, 60 µg/ml penicillin, 50 µg/ml streptomycin, and 50 µg/ml gentamicin sulfate (complete DMEM/F-12 medium) in a humidified atmosphere with 5% CO_2 at 37 °C.

Treatment of CHO-K1 Cells with Metabolic Inhibitors of Sphingolipid Biosynthesis

CHO-K1 cells were grown in complete DMEM/F-12 medium for ~ 24 h followed by treatment with increasing concentrations of FB_1 or myriocin for ~ 60–66 h in DMEM/F-12 medium containing 5% (v/v) FCS in a humidified atmosphere with 5% CO_2 at 37 °C. In case of PDMP treatment, cells were subjected to 48 h treatment with increasing concentrations of PDMP in lipid-deficient Nutridoma-BO medium [DMEM/F-12 medium containing 1% (v/v) Nutridoma-SP, 0.33 mg/ml oleic acid-albumin complex, and 0.1% (v/v) FCS] in a humidified atmosphere with 5% CO_2 at 37 °C. Stock solutions of FB_1 and PDMP were prepared in water, whereas stock solution of myriocin was prepared in DMSO.

Cell Viability Assay

The viability of CHO-K1 cells upon treatment with metabolic inhibitors of sphingolipid biosynthesis was assessed using MTT assay as described previously (Rao et al. 2021). Briefly, cells were plated in 96-well plates and treated with increasing concentrations of FB_1, myriocin, or PDMP. Cells were subsequently incubated with MTT dissolved in serum-free DMEM/F-12 medium at a final concentration of 0.4 mg/ml at 37 °C for 1 h. Reduction of MTT salt by mitochondrial enzymes in cells (Vistica et al. 1991) led to formation of formazan crystals which were dissolved in DMSO and the color obtained was measured by absorbance at 540 nm in a Multiskan Spectrum Plate Reader (Thermo Fisher Scientific, Rochester, NY).

Cell Lysate Preparation

After treatment with various inhibitors, cells were harvested using 0.1% (w/v) trypsin/EDTA and resuspended in PBS. Cells were subsequently sonicated using VCX 500 Vibracell sonics (Newtown, CT) sonicator for 5 min using 10 s on and 10 s off cycles at an amplitude of ~ 20%. Total protein concentration of cell lysates was determined using the BCA assay reagent (Smith et al. 1985).

Estimation of Lipid Content by Thin Layer Chromatography (TLC)

Total lipid extraction from cell lysates obtained from control and cells treated with metabolic inhibitors was performed according to the Bligh and Dyer method (Bligh and Dyer 1959). Lipid extracts from 0.5 mg (for FB_1 and myriocin-treated cells) or 3 mg (for PDMP-treated cells) protein were dried under a stream of nitrogen at ~ 45 °C, and the dried lipids were subsequently dissolved in chloroform/methanol (1:1, v/v). The extracted lipids were separated by TLC on precoated silica TLC plate using chloroform/methanol/0.22% (w/v) aqueous $CaCl_2$ (60:35:8, v/v/v) as a solvent system (Dragusin et al. 2003). A sphingomyelin standard was run to identify the sphingomyelin band in lipid extracts obtained from FB_1 and myriocin-treated cells. Neutral glycosphingolipid mixture was used as a standard to identify the glycosphingolipid bands in PDMP-treated cells. The separated lipids were visualized by charring with a solution containing cupric sulfate (10%, w/v) and phosphoric acid (8%, v/v) at ~ 150 °C (Baron and Coburn 1984). The TLC plates were scanned and lipid band intensities were quantified based on densitometric analysis using Adobe Photoshop (version 10.0, Adobe Systems, San Jose, CA). Intensities of the sphingomyelin and glycosphingolipid bands in sphingolipid-depleted cells were normalized to the intensity of the respective bands from control cells.

Flow Cytometric Analysis of CHO-K1 Cells

Following treatment with metabolic inhibitors of sphingolipid biosynthesis, cells were harvested using 0.1% (w/v) trypsin/EDTA, suspended in PBS, and spun down for 3 min at 600×*g*. Cells were fixed with ice-cold 70% (v/v) ethanol for 10 min and subsequently spun down for 3 min at 600×*g*. Fixed cells were washed twice with PBS and labeled with 50 µg/ml propidium iodide for 15 min at ~ 4 °C in the presence of 200 µg/ml RNase A in PBS containing 2% (v/v) FCS. Propidium iodide is a popular DNA binding fluorescent dye used for quantitating cellular DNA content in fixed cells. After labeling, cells were spun down for 3 min at 600×*g* and pelleted cells were washed and resuspended in PBS containing 2% (v/v) FCS. Distribution of cells in different phases of the cell cycle was monitored in a Gallios (Beckman Coulter, Brea, CA) [or BD LSRFortessa (Franklin Lakes, NJ)] flow cytometer using propidium iodide fluorescence. To distinguish single cells from multiplets of cells, we

used a 'pulse processing' protocol where fluorescence from multiplets of cells was excluded using fluorescence pulse width and fluorescence pulse area display (see Fig. 2a) and 10,000 events were recorded for each experiment. Propidium iodide was excited with 488 nm (or 561 nm) laser and its fluorescence was collected using 620/30 nm (or 585/15 nm) bandpass filter. A representative flow cytometry histogram of fixed CHO-K1 cells upon propidium iodide labeling with a schematic of sequential phases of cell cycle as an inset is shown in Fig. 2b. Kaluza analysis software (version 1.5a, Beckman Coulter, Brea, CA) [or BD FACSDiva software (version 8.0.2, Franklin Lakes, NJ)] was used to acquire data and Kaluza analysis software (version 1.5a, Beckman Coulter, Brea, CA) was used to analyze data.

Statistical Analysis

Significance levels were calculated using two-tailed unpaired *t*-test with 95% confidence interval using GraphPad Prism software (version 4.0, San Diego, CA). All plots were generated using Microcal Origin (version 9.7, OriginLab, Northampton, MA).

Results

We used three metabolic inhibitors (myriocin, FB_1, and PDMP) which induce a block at precise steps in the sphingolipid biosynthetic pathway (Delgado et al. 2006) for metabolically depleting sphingolipids from CHO-K1 cells. Myriocin, also known as ISP-1 or thermozymocidin, is a fungal metabolite that acts as a competitive inhibitor of the enzyme serine palmitoyltransferase which is responsible for the synthesis of 3-ketosphinganine (Lee et al. 2012). FB_1 is a potent fungal mycotoxin obtained from *Fusarium* species (Stockmann-Juvala and Savolainen 2008). FB_1 exhibits structural similarity with sphingoid bases and acts as a competitive inhibitor of the enzyme ceramide synthase (*N*-acetyltransferase), which catalyzes the acylation of sphinganine in de novo sphingolipid biosynthesis and reutilization of sphingosine obtained from sphingolipid turnover (Wang et al. 1991; Voss and Riley 2013). PDMP is a synthetic analog of ceramide which acts as a competitive inhibitor of the enzyme glucosylceramide synthase (Inokuchi and Radin 1987).

Metabolic Depletion by FB_1 Does Not Alter Cell Cycle Progression

In order to explore the role of sphingolipids in cell cycle progression, we first treated CHO-K1 cells with FB_1 to metabolically deplete cellular sphingolipids. FB_1 is the most abundant among the family of fumonisins (Marasas 1995; Stockmann-Juvala and Savolainen 2008), a group of fungal mycotoxins which act as a competitive inhibitor of the enzyme ceramide synthase that catalyzes the acylation of either sphinganine or sphingosine (Wang et al. 1991; Voss and Riley 2013). Treatment with FB_1 could induce oxidative stress and cytotoxicity at high concentrations (Fornelli et al. 2004; Kouadio et al. 2005). We therefore carefully chose the concentration range of FB_1 to ensure that cell viability was not compromised in our experiments. For this, we used MTT assay to assess the viability of CHO-K1 cells treated with increasing concentrations of FB_1 (see Fig. 3a). We observed that the highest concentration of FB_1 at which cells remained viable was 40 μM (Fig. 3a). The concentration of FB_1 used in this work therefore never exceeded 40 μM. Next, we estimated sphingolipid content of cells from total lipids extracted from cell lysates of control and FB_1-treated cells and separated using thin layer chromatography. Since sphingomyelin represents the major fraction of total cellular sphingolipids (Gault et al. 2010; van Meer and de Kroon 2011), we quantitated cellular sphingomyelin content as a representative indicator of total sphingolipids. A representative thin layer chromatogram showing sphingomyelin content in control and FB_1-treated cells is shown in Fig. 3b. The sphingomyelin band intensities were analyzed using densitometric analysis of the chromatogram as described in Materials and Methods and are shown in Fig. 3c. We chose two representative concentrations [i.e., the lowest (10 μM) and highest (40 μM)] of FB_1 for quantifying reduction of cellular sphingomyelin under FB_1-treated conditions. As shown in Fig. 3b, upon treatment of cells with 10 and 40 μM of FB_1, we observed a dose-dependent reduction in membrane sphingomyelin content which is quantified and shown in Fig. 3c. Treatment of cells with 10 μM FB_1 resulted in a reduction in membrane sphingomyelin content by ~ 53% relative to control (untreated) cells. At the highest concentration (40 μM) of FB_1, we observed ~ 65% reduction in sphingomyelin content.

Following this, we monitored the effect of sphingolipid depletion by FB_1 treatment upon cell cycle progression utilizing flow cytometry. The phases of cell cycle could be identified on the basis of changes in cellular DNA content in a population of cells using flow cytometry. Figure 2b shows a typical flow cytometry histogram for asynchronous CHO-K1 cells acquired upon propidium iodide labeling. The histogram depicts the distribution of cells in G1 (blue), S (red), and G2/M (green) phases of the cell cycle. In order to estimate the effect of FB_1 in a concentration-dependent manner, we determined distribution of cells (*i.e.*, number of cells in G1, S, and G2/M phases) with increasing concentrations of FB_1 and plotted in Fig. 3d. The figure shows that the distribution of control cells in G1, S, and G2/M phases was ~ 54, ~ 24, and ~ 20%, respectively. Interestingly, there is no significant change in the distribution of cell numbers across G1, S, and G2/M phases of the cell cycle even upon

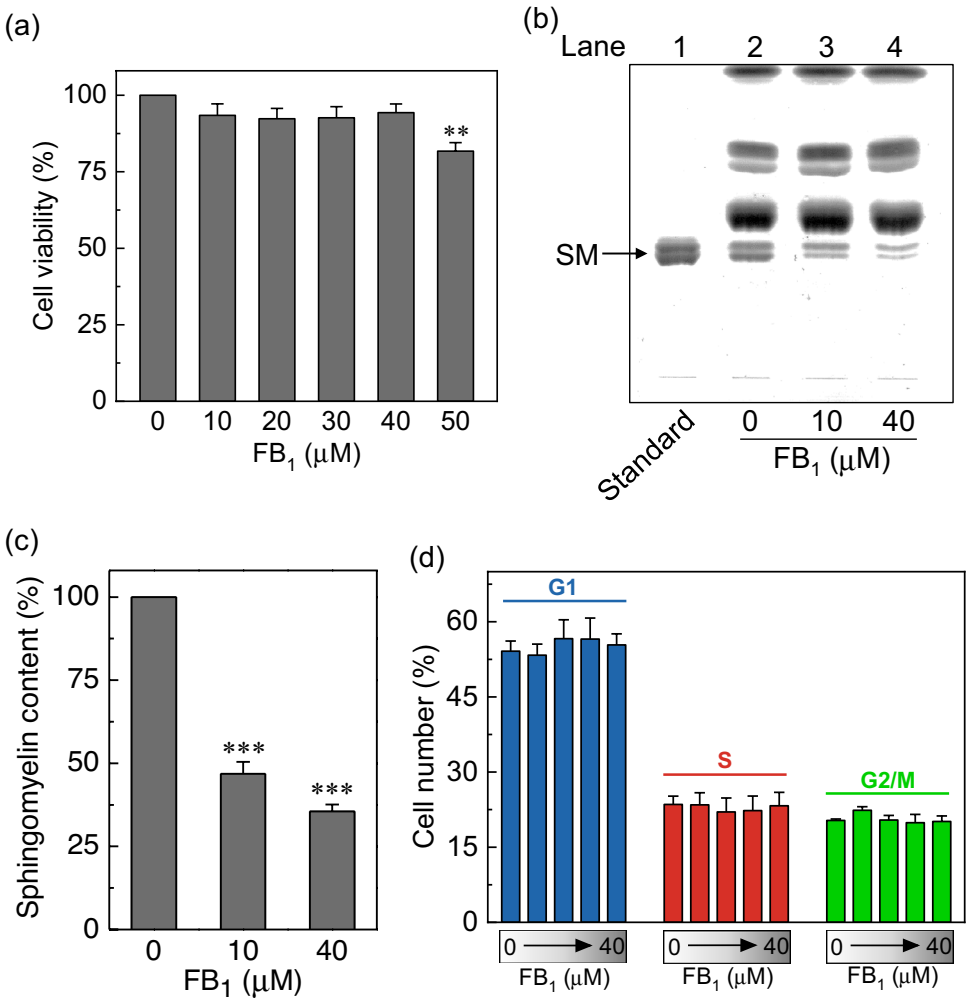

Fig. 3 Effect of FB_1 treatment on sphingolipid content and cell cycle progression in CHO-K1 cells. **a** The viability of CHO-K1 cells was assessed by MTT assay upon treatment with increasing concentrations of FB_1, ranging from 10 to 50 μM. Values are expressed as percentages of cell viability normalized to control cells (without FB_1 treatment). Data represent means ± SE from three independent experiments (**corresponds to significant difference ($p < 0.01$) in cell viability in 50 μM FB_1-treated cells relative to untreated cells). **b** A representative thin layer chromatogram showing lipids extracted from cell lysates of control and FB_1-treated cells. Lane 2 shows lipids extracted from control cells, whereas lanes 3 and 4 show lipids extracted from cells treated with 10 and 40 μM FB_1, respectively. The position of the sphingomyelin (SM) bands were identified by using a standard in lane 1 (shown with an arrow). **c** Sphingomyelin content quantitated by densitometric analysis of the chromatogram. Values are expressed as percentages of sphingomyelin content normalized to control cells. Data represent means ± SE from three independent experiments (***corresponds to significant ($p < 0.001$) difference in sphingomyelin content in 10 and 40 μM FB_1-treated cells relative to control cells). **d** Distribution of cells in various cell cycle phases upon FB_1 treatment. Number of cells in G1 (blue), S (red), and G2/M (green) phases of the cell cycle in control cells and cells treated with 10, 20, 30, and 40 μM FB_1 are shown. See Materials and methods for more details

treatment with 40 μM FB_1 (Fig. 3d). Our results therefore suggest that metabolic depletion of sphingolipids by FB_1 does not modulate cell cycle progression in CHO-K1 cells.

Myriocin Treatment Does Not Change Cell Cycle Progression

In order to further explore the effect of metabolic inhibition of sphingolipids on cell cycle progression, we utilized a proximal inhibitor (myriocin) of sphingolipid biosynthetic pathway. Myriocin is a fungal metabolite that acts as a competitive inhibitor of the enzyme serine palmitoyltransferase, which catalyzes the rate-limiting step in the sphingolipid biosynthetic pathway and leads to synthesis of 3-ketosphinganine that is converted to sphinganine (Lee et al. 2012). To determine the viability of CHO-K1 cells upon myriocin treatment, we performed MTT viability assay and observed that cells remained viable upon treatment with up to 1 μM myriocin (Fig. 4a). To estimate the sphingolipid content under these conditions, we

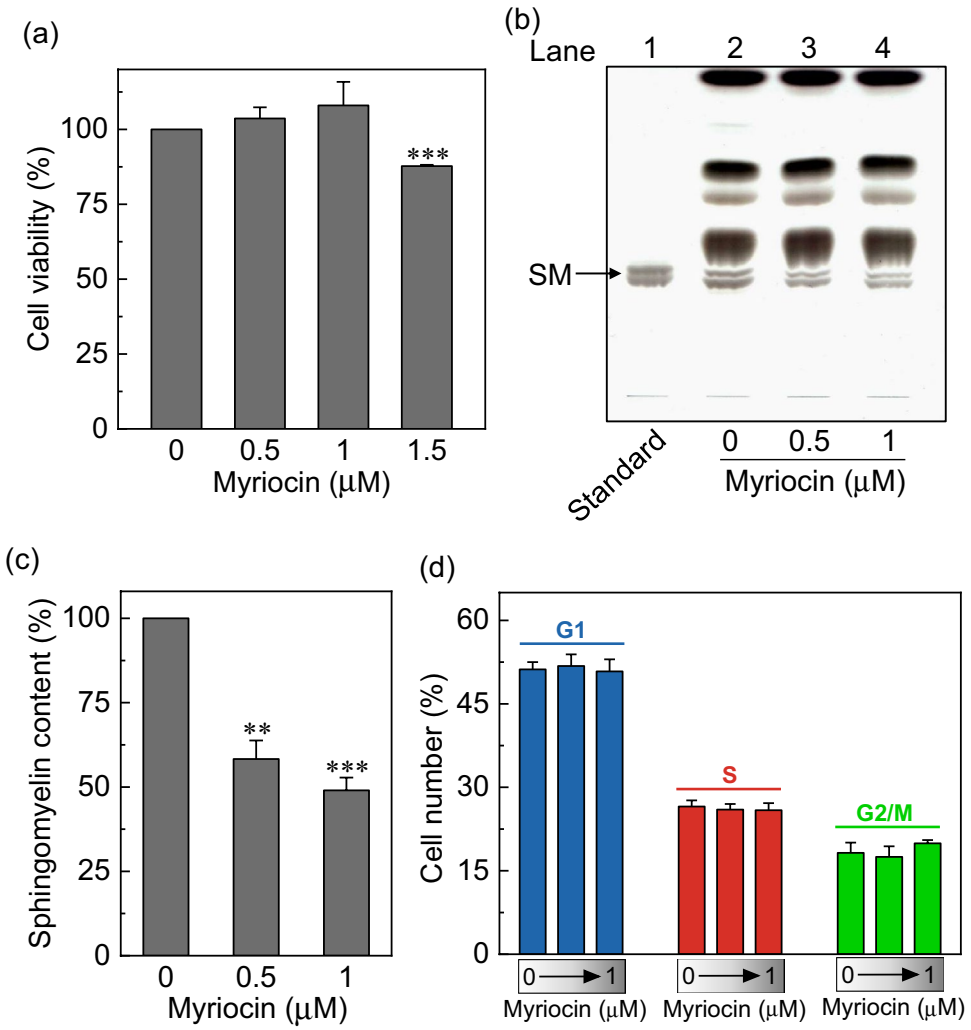

Fig. 4 Effect of myriocin treatment on sphingolipid content and cell cycle progression in CHO-K1 cells. **a** Viability of CHO-K1 cells was assessed by MTT assay upon treatment with increasing concentrations of myriocin. Values are expressed as percentages of viability normalized to control cells (without myriocin treatment). Data represent means ± SE from three independent experiments (***corresponds to significant difference ($p < 0.001$) in cell viability in 1.5 μM myriocin-treated cells relative to untreated cells). **b** A representative thin layer chromatogram showing lipids extracted from cell lysates of control and myriocin-treated cells. Lane 2 shows lipids extracted from control cells, whereas lanes 3 and 4 show lipids extracted from cells treated with 0.5 and 1 μM myriocin, respectively. The position of the sphingomyelin (SM) bands were identified by using a standard in lane 1 (shown with an arrow). **c** Sphingomyelin content was quantified by densitometric analysis of the chromatogram. Values are expressed as percentages of sphingomyelin content normalized to control cells. Data represent means ± SE from three independent experiments (**and *** correspond to significant ($p < 0.01$ and $p < 0.001$) difference in sphingomyelin content in cells treated with 0.5 and 1 μM myriocin, respectively, relative to control cells). **d** Distribution of cells in various cell cycle phases upon treatment with myriocin. Number of cells in G1 (blue), S (red), and G2/M (green) phases of the cell cycle in control cells and cells treated with 0.5 and 1 μM myriocin are shown. See Materials and methods for other details

quantitated cellular sphingomyelin content as described earlier. A representative thin layer chromatogram showing sphingomyelin content in control and myriocin-treated cells is shown in Fig. 4b. As shown in the figure, treatment with increasing concentrations of myriocin led to concentration-dependent reduction in membrane sphingomyelin content. Sphingomyelin band intensities were analyzed from the chromatogram and the sphingomyelin content upon myriocin treatment is shown in Fig. 4c. Treatment of cells with 0.5 and 1 μM myriocin resulted in a significant reduction in membrane sphingomyelin content by ~ 42% and ~ 51% relative to control (untreated) cells. We subsequently explored the effect of sphingolipid depletion by myriocin on distribution of cells in various cell cycle phases. Our results showed no significant change in the number of cells across the G1, S, and G2/M phases of the cell cycle upon treatment with increasing concentrations of myriocin (Fig. 4d). This suggests that metabolic depletion

of sphingolipids, even at the first step in its biosynthetic pathway, did not lead to changes in cell cycle progression.

Treatment with PDMP Does Not Alter Cell Cycle Progression

Subsequent to observing no change in cell cycle progression upon treatment with FB_1 and myriocin, we explored the effect of metabolic depletion of sphingolipids in a distal step of the biosynthetic pathway. For this, we used PDMP, a synthetic analog of ceramide which leads to inhibition in the production of glucosylceramide and complex glycosphingolipids (Inokuchi and Radin 1987). We determined the viability of CHO-K1 cells upon treatment with increasing concentrations of PDMP and observed that cells remained viable upon treatment with up to 15 µM PDMP (Fig. 5a). To estimate the sphingolipid content under these conditions, we quantitated cellular glycosphingolipid content by TLC

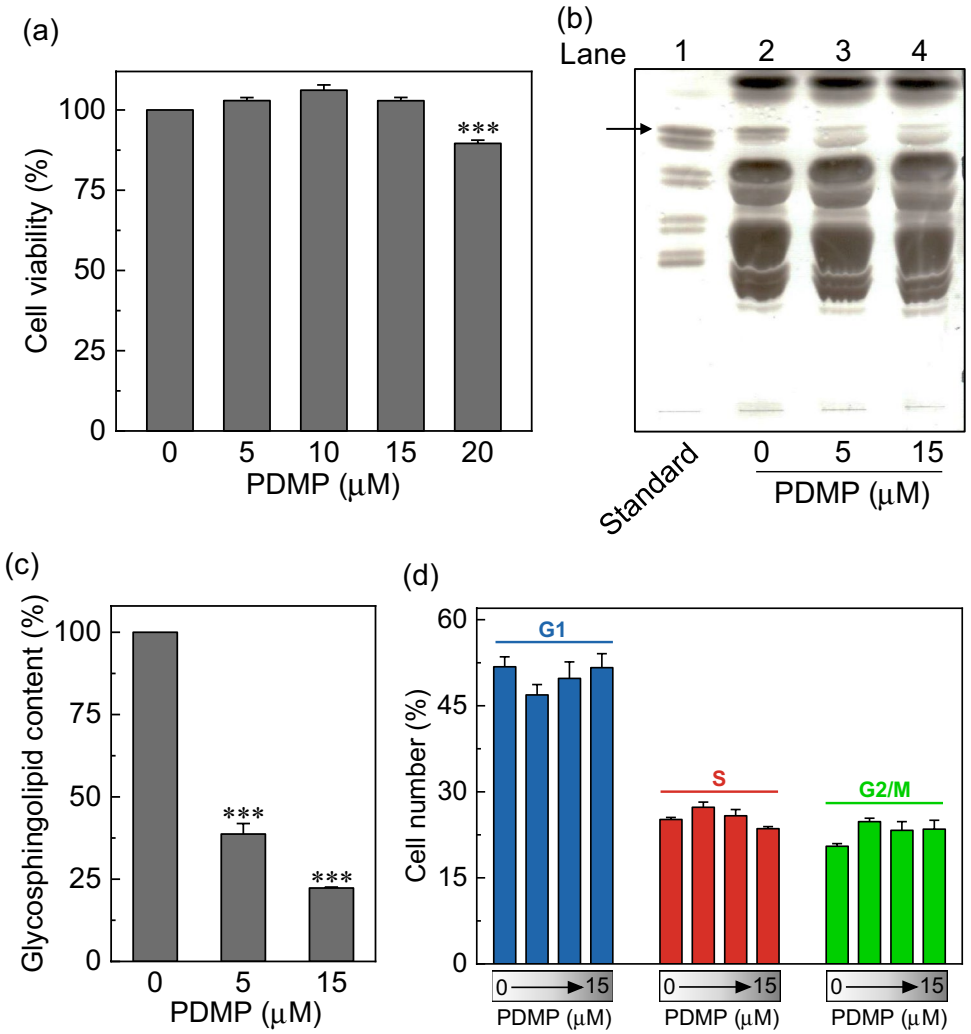

Fig. 5 Effect of PDMP treatment on glycosphingolipid content and cell cycle progression in CHO-K1 cells. **a** Viability of CHO-K1 cells was determined by MTT assay upon treatment with increasing concentrations of PDMP. Values are expressed as percentages of cell viability normalized to control cells (without PDMP treatment). Data represent means ± SE from three independent experiments (***corresponds to significant difference ($p < 0.001$) in cell viability in 20 µM PDMP-treated cells relative to untreated cells). **b** A representative thin layer chromatogram showing lipids extracted from cell lysates of control and PDMP-treated cells. Lane 2 shows lipids extracted from control cells, whereas lanes 3 and 4 show lipids extracted from cells treated with 5 and 15 µM PDMP, respectively. The position of the glycosphingolipid band was identified by using a standard in lane 1 (shown with an arrow). **c** Glycosphingolipid content was quantified by densitometric analysis of the chromatogram. Values are expressed as percentages of glycosphingolipid content normalized to control cells. Data represent means ± SE from three independent experiments (***corresponds to significant ($p < 0.001$) difference in glycosphingolipid content in cells treated with 5 and 15 µM PDMP relative to control cells). **d** Distribution of cells in various cell cycle phases upon treatment with PDMP. Number of cells in G1 (blue), S (red), and G2/M (green) phases of the cell cycle in control cells and cells treated with 5, 10, and 15 µM PDMP are shown. See Materials and methods for more details

using two representative concentrations of PDMP (5 and 15 μM) from the concentration range determined by MTT assay (Fig. 5b). For identifying glycosphingolipids in lipids isolated from control and PDMP-treated cells, we used a standard containing neutral glycosphingolipid mixture and observed a prominent dose-dependent reduction of a glycosphingolipid band identified using the standard in lane 1 (see Fig. 5b). The glycosphingolipid band intensities were quantified from the chromatogram and are shown in Fig. 5c. Treatment of cells with 5 and 15 μM PDMP resulted in a significant reduction in the glycosphingolipid content by ~ 61% and ~ 78% relative to control (untreated) cells. Following this, we monitored the effect of sphingolipid depletion by PDMP upon distribution of cells in various cell cycle phases. Our results showed that the distribution in number of cells across G1, S, and G2/M phases of the cell cycle remained invariant upon treatment with PDMP, even at the highest concentration (Fig. 5d). These results indicate that depletion of cellular glycosphingolipids using PDMP does not induce changes in cell cycle progression in CHO-K1 cells.

Discussion

Sphingomyelin is the major sphingolipid in eukaryotes which acts as a reservoir for bioactive molecules such as ceramide, sphingosine, and sphingosine-1-phosphate (Bartke and Hannun 2009). Bioactive sphingolipids play an essential role in regulating key physiological processes which includes cell growth, migration, inflammation, intracellular trafficking, and cancer pathogenesis (Jayadev et al. 1995; Hannun 1996; Ogretmen and Hannun 2004; Acharya et al. 2008; Gangoiti et al. 2008; Hannun and Obeid 2008; Morad and Cabot 2013; Adada et al. 2014). One of the mechanisms by which sphingolipids orchestrate the regulation of diverse signaling pathways is through formation of membrane microdomains (Aureli et al. 2015; Grassi et al. 2020). Importantly, sphingolipids and cholesterol have been proposed to cluster together to form membrane domains which function as platforms for lateral segregation of proteins during their trafficking in cells and in the process of signal transduction (Brown 1998). Cholesterol has been suggested to modulate the fluidity of sphingolipid domains and help in their segregation for proper function. The interaction of cholesterol with sphingolipids depends on molecular properties of the specific sphingolipid, with small headgroup size of the sphingolipid exerting a destabilizing effect on cholesterol-sphingolipid interaction (Ramstedt and Slotte 2006). Sphingomyelin levels were shown to affect cholesterol dynamics (Slotte and Bierman 1988) and play a key role in cholesterol retention in plasma membranes during cholesterol depletion using cyclodextrin-type carriers (Fukasawa et al. 2000). Sphingomyelinase-induced disruption of liquid-ordered phase membranes leads to displacement of cholesterol from liquid-ordered to the fluid phase (Taniguchi et al. 2006). In addition, cholesterol can be displaced by ceramide in liquid-ordered phase membranes which could regulate the formation of membrane domains (Alanko et al. 2005; Goñi and Alonso 2009).

Such an interplay between sphingolipids and cholesterol could affect not only membrane domain formation but could also have consequences on other crucial physiological processes such as cell division. We have previously shown that cholesterol content could vary across cell cycle stages (Singh et al. 2013; Sarkar et al. 2020) and inhibition of cholesterol biosynthesis leads to cell cycle arrest in the G1 phase (Singh et al. 2013). Considering the close functional association of sphingolipids with cholesterol and the crucial role of sphingolipid metabolism in cell division processes (Fridberg et al. 2008; Epstein et al. 2012; Castro et al. 2013) as well as cancer (Ogretmen and Hannun 2004; Gangoiti et al. 2008; Ogretmen 2018; Medatwal et al. 2020; Pani et al. 2021), we explored the effect of metabolic depletion of sphingolipids on cell distribution in specific cell cycle phases. Our results show that although metabolic inhibitors resulted in considerable reduction in specific sphingolipids, such inhibition in sphingolipid biosynthesis did not lead to significant modulation in cell cycle progression in CHO-K1 cells. It should be noted that the sphingolipid content in CHO cells is relatively low compared to other cell types (Hooghwinkel et al. 1969; Warnock et al. 1993). In addition, a recent study has reported that the content and diversity of sphingolipids in ovary is less relative to other cell types from murine tissues (Muralidharan et al. 2021). It is possible that cell cycle progression could depend on sphingolipid content specific to individual cell types and adequate caution may be exercised while interpreting experimental results in relation to cell types.

Previous reports have shown the modulation in cell cycle progression in normal and cancer cells upon treatment with FB_1 (Ciacci-Zanella et al. 1998; Mobio et al. 2000; Marin et al. 2007; Wang et al. 2014), myriocin (Lee et al. 2011), and PDMP (Rani et al. 1995; Dijkhuis et al. 2006). Since bioactive sphingolipids are either upregulated or downregulated in cancer cells (Ogretmen 2006; Ryland et al. 2011; Hannun and Obeid 2018), it is challenging to determine the various factors implicated in multiple functions mediated by sphingolipids in each cell type. Such fine-tuned interplay of sphingolipid metabolism could be involved in the modulation of cell cycle progression in specific cell types, with cancer cells being more susceptible to loss in cellular homeostasis upon disruption in sphingolipid metabolism. Interestingly, sphingolipids (Saddoughi et al. 2008; Shaw et al. 2018) and membrane domains (Codini et al. 2021) could act as attractive targets for developing innovative therapeutic strategies for cancer. We envision that future studies using

cancer cells could augment our understanding on the role of sphingolipids in cell cycle progression and provide better insight into lipid-dependent cell cycle associated processes.

Acknowledgements This work was supported by SERB Distinguished Fellowship Grant (Department of Science and Technology, Govt. of India) to A.C. and core support from CSIR-Centre for Cellular and Molecular Biology. B.D.R. and P.S. were supported as Project Associate and Senior Project Associate, respectively, by a CSIR FBR Grant to A.C. (MLP 0146). We thank Gunda Srinivas for help with acquiring flow cytometric data and members of the Chattopadhyay laboratory for critically reading the manuscript and for their comments.

Data Availability The datasets generated during and/or analyzed during the current study are available from the corresponding author on reasonable request.

Declarations

Conflict of interest The authors declare that they have no conflicts of interest.

References

Acharya JK, Dasgupta U, Rawat SS, Yuan C, Sanxaridis PD, Yonamine I, Karim P, Nagashima K, Brodsky MH, Tsunoda S, Acharya U (2008) Cell-nonautonomous function of ceramidase in photoreceptor homeostasis. Neuron 57:69–79

Adada M, Canals D, Hannun YA, Obeid LM (2014) Sphingolipid regulation of ezrin, radixin, and moesin proteins family: implications for cell dynamics. Biochim Biophys Acta 1841:727–737

Alanko SMK, Halling KK, Maunula S, Slotte JP, Ramstedt B (2005) Displacement of sterols from sterol/sphingomyelin domains in fluid bilayer membranes by competing molecules. Biochim Biophys Acta 1715:111–121

Aureli M, Grassi S, Prioni S, Sonnino S, Prinetti A (2015) Lipid membrane domains in the brain. Biochim Biophys Acta 1851:1006–1016

Baier CJ, Barrantes FJ (2007) Sphingolipids are necessary for nicotinic acetylcholine receptor export in the early secretory pathway. J Neurochem 101:1072–1084

Barnum KJ, O'Connell MJ (2014) Cell cycle regulation by checkpoints. Methods Mol Biol 1170:29–40

Baron CB, Coburn RF (1984) Comparison of two copper reagents for detection of saturated and unsaturated neutral lipids by charring densitometry. J Liq Chromatogr 7:2793–2801

Bartke N, Hannun YA (2009) Bioactive sphingolipids: metabolism and function. J Lipid Res 50:S91–S96

Bligh EG, Dyer WJ (1959) A rapid method of total lipid extraction and purification. Can J Biochem Physiol 37:911–917

Brown RE (1998) Sphingolipid organization in biomembranes: what physical studies of model membranes reveal. J Cell Sci 111:1–9

Castro EV, Yoneyama KG, Haapalainen EF, Toledo MS, Takahashi HK, Straus AH (2013) Myriocin, a serine palmitoyltransferase inhibitor, blocks cytokinesis in *Leishmania (Viannia) braziliensis* promastigotes. J Eukaryot Microbiol 60:377–387

Ciacci-Zanella JR, Merrill AH Jr, Wang E, Jones C (1998) Characterization of cell-cycle arrest by fumonisin B_1 in CV-1 cells. Food Chem Toxicol 36:791–804

Codini M, Garcia-Gil M, Albi E (2021) Cholesterol and sphingolipid enriched lipid rafts as therapeutic targets in cancer. Int J Mol Sci 22:726

Dart C (2010) Lipid microdomains and the regulation of ion channel function. J Physiol 588:3169–3178

Delgado A, Casas J, Llebaria A, Abad JL, Fabrias G (2006) Inhibitors of sphingolipid metabolism enzymes. Biochim Biophys Acta 1758:1957–1977

Dijkhuis A-J, Klappe K, Jacobs S, Kroesen B-J, Kamps W, Sietsma H, Kok JW (2006) PDMP sensitizes neuroblastoma to paclitaxel by inducing aberrant cell cycle progression leading to hyperploidy. Mol Cancer Ther 5:593–601

Dragusin M, Gurgui C, Schwarzmann G, Hoernschemeyer J, van Echten-Deckert G (2003) Metabolism of the unnatural anticancer lipid safingol, L-*threo*-dihydrosphingosine, in cultured cells. J Lipid Res 44:1772–1779

Epstein S, Castillon GA, Qin Y, Riezman H (2012) An essential function of sphingolipids in yeast cell division. Mol Microbiol 84:1018–1032

Fantini J (2003) How sphingolipids bind and shape proteins: molecular basis of lipid-protein interactions in lipid shells, rafts and related biomembrane domains. Cell Mol Life Sci 60:1027–1032

Fantini J, Barrantes FJ (2009) Sphingolipid/cholesterol regulation of neurotransmitter receptor conformation and function. Biochim Biophys Acta 1788:2345–2361

Fornelli F, Minervini F, Mulè G (2004) Cytotoxicity induced by nivalenol, deoxynivalenol, and fumonisin B_1 in the SF-9 insect cell line. In Vitro Cell Dev Biol Anim 40:166–171

Fridberg A, Olson CL, Nakayasu ES, Tyler KM, Almeida IC, Engman DM (2008) Sphingolipid synthesis is necessary for kinetoplast segregation and cytokinesis in *Trypanosoma brucei*. J Cell Sci 121:522–535

Fukasawa M, Nishijima M, Hanada K (1999) Genetic evidence for ATP-dependent endoplasmic reticulum-to-Golgi apparatus trafficking of ceramide for sphingomyelin synthesis in Chinese Hamster Ovary cells. J Cell Biol 144:673–685

Fukasawa M, Nishijima M, Itabe H, Takano T, Hanada K (2000) Reduction of sphingomyelin level without accumulation of ceramide in Chinese Hamster Ovary cells affects detergent-resistant membrane domains and enhances cellular cholesterol efflux to methyl-β-cyclodextrin. J Biol Chem 275:34028–34034

Gangoiti P, Granado MH, Alonso A, Goñi FM, Gómez-Muñoz A (2008) Implication of ceramide, ceramide 1-phosphate and sphingosine 1-phosphate in tumorigenesis. Transl Oncogenom 3:81–98

García-Arribas AB, Alonso A, Goñi FM (2016) Cholesterol interactions with ceramide and sphingomyelin. Chem Phys Lipids 199:26–34

Gault CR, Obeid LM, Hannun YA (2010) An overview of sphingolipid metabolism: from synthesis to breakdown. Adv Exp Med Biol 688:1–23

Goñi FM, Alonso A (2009) Effects of ceramide and other simple sphingolipids on membrane lateral structure. Biochim Biophys Acta 1788:169–177

Grassi S, Giussani P, Mauri L, Prioni S, Sonnino S, Prinetti A (2020) Lipid rafts and neurodegeneration: structural and functional roles in physiologic aging and neurodegenerative diseases. J Lipid Res 61:636–654

Hannun YA (1996) Functions of ceramide in coordinating cellular responses to stress. Science 274:1855–1859

Hannun YA, Obeid LM (2008) Principles of bioactive lipid signalling: lessons from sphingolipids. Nat Rev Mol Cell Biol 9:139–150

Hannun YA, Obeid LM (2018) Sphingolipids and their metabolism in physiology and disease. Nat Rev Mol Cell Biol 19:175–191

Harper JV, Brooks G (2005) The mammalian cell cycle: an overview. Methods Mol Biol 296:113–153

Holthuis JCM, Pomorski T, Raggers RJ, Sprong H, Van Meer G (2001) The organizing potential of sphingolipids in intracellular membrane transport. Physiol Rev 81:1689–1723

Hooghwinkel GJM, van Gelderen HH, Staal A (1969) Sphingomyelin of red blood cells in lipidosis and in dementia of unknown origin in children. Arch Dis Child 44:197–202

Hussain G, Wang J, Rasul A, Anwar H, Imran A, Qasim M, Zafar S, Kamran SKS, Razzaq A, Aziz N, Ahmad W, Shabbir A, Iqbal J, Baig SM, Sun T (2019) Role of cholesterol and sphingolipids in brain development and neurological diseases. Lipids Health Dis 18:26

Inokuchi J-I, Radin NS (1987) Preparation of the active isomer of l-phenyl-2-decanoylamino-3-morpholino-1-propanol, inhibitor of murine glucocerebroside synthetase. J Lipid Res 28:565–571

Jafurulla M, Chattopadhyay A (2015) Sphingolipids in the function of G protein-coupled receptors. Eur J Pharmacol 763:241–246

Jafurulla M, Bandari S, Pucadyil TJ, Chattopadhyay A (2017) Sphingolipids modulate the function of human serotonin$_{1A}$ receptors: insights from sphingolipid-deficient cells. Biochim Biophys Acta 1859:598–604

Jayadev S, Liu B, Bielawska AE, Lee JY, Nazaire F, Pushkareva MY, Obeid LM, Hannun YA (1995) Role for ceramide in cell cycle arrest. J Biol Chem 270:2047–2052

Klemm RW, Ejsing CS, Surma MA, Kaiser H-J, Gerl MJ, Sampaio JL, de Robillard Q, Ferguson C, Proszynski TJ, Shevchenko A, Simons K (2009) Segregation of sphingolipids and sterols during formation of secretory vesicles at the trans-Golgi network. J Cell Biol 185:601–612

Kouadio JH, Mobio TA, Baudrimont I, Moukha S, Dano SD, Creppy EE (2005) Comparative study of cytotoxicity and oxidative stress induced by deoxynivalenol, zearalenone or fumonisin B$_1$ in human intestinal cell line Caco-2. Toxicology 213:56–65

Lange Y, Swaisgood MH, Ramos BV, Steck TL (1989) Plasma membranes contain half the phospholipid and 90% of the cholesterol and sphingomyelin in cultured human fibroblasts. J Biol Chem 264:3786–3793

Lee Y-S, Choi K-M, Choi M-H, Ji S-Y, Lee S, Sin D-M, Oh K-W, Lee Y-M, Hong J-T, Yun Y-P, Yoo HS (2011) Serine palmitoyltransferase inhibitor myriocin induces growth inhibition of B16F10 melanoma cells through G$_2$/M phase arrest. Cell Prolif 44:320–329

Lee Y-S, Choi K-M, Lee S, Sin D-M, Yoo K-S, Lim Y, Lee Y-M, Hong J-T, Yun Y-P, Yoo H-S (2012) Myriocin, a serine palmitoyltransferase inhibitor, suppresses tumor growth in a murine melanoma model by inhibiting de novo sphingolipid synthesis. Cancer Biol Ther 13:92–100

Mahfoud R, Garmy N, Maresca M, Yahi N, Puigserver A, Fantini J (2002) Identification of a common sphingolipid-binding domain in Alzheimer, prion, and HIV-1 proteins. J Biol Chem 277:11292–11296

Marasas WFO (1995) Fumonisins: their implications for human and animal health. Nat Toxins 3:193–198

Marin DE, Gouze M-E, Taranu I, Oswald IP (2007) Fumonisin B1 alters cell cycle progression and interleukin-2 synthesis in swine peripheral blood mononuclear cells. Mol Nutr Food Res 51:1406–1412

Medatwal N, Ansari MN, Kumar S, Pal S, Jha SK, Verma P, Rana K, Dasgupta U, Bajaj A (2020) Hydrogel-mediated delivery of celastrol and doxorubicin induces a synergistic effect on tumor regression *via* upregulation of ceramides. Nanoscale 12:18463

Mobio TA, Anane R, Baudrimont I, Carratú M-R, Shier TW, Dano SD, Ueno Y, Creppy EE (2000) Epigenetic properties of fumonisin B$_1$: cell cycle arrest and DNA base modification in C6 glioma cells. Toxicol Appl Pharmacol 164:91–96

Morad SAF, Cabot MC (2013) Ceramide-orchestrated signalling in cancer cells. Nat Rev Cancer 13:51–65

Muralidharan S, Shimobayashi M, Ji S, Burla B, Hall MN, Wenk MR, Torta F (2021) A reference map of sphingolipids in murine tissues. Cell Rep 35:109250

Ogretmen B (2006) Sphingolipids in cancer: regulation of pathogenesis and therapy. FEBS Lett 580:5467–5476

Ogretmen B (2018) Sphingolipid metabolism in cancer signalling and therapy. Nat Rev Cancer 18:33–50

Ogretmen B, Hannun YA (2004) Biologically active sphingolipids in cancer pathogenesis and treatment. Nat Rev Cancer 4:604–616

Olsen ASB, Færgeman NJ (2017) Sphingolipids: membrane microdomains in brain development, function and neurological diseases. Open Biol 7:170069

Paila YD, Ganguly S, Chattopadhyay A (2010) Metabolic depletion of sphingolipids impairs ligand binding and signaling of human serotonin$_{1A}$ receptors. Biochemistry 49:2389–2397

Pani T, Rajput K, Kar A, Sharma H, Basak R, Medatwal N, Saha S, Dev G, Kumar S, Gupta S, Mukhopadhyay A, Malakar D, Maiti TK, Arimbasseri AG, Deo SVS, Sharma RD, Bajaj A, Dasgupta U (2021) Alternative splicing of *ceramide synthase 2* alters levels of specific ceramides and modulates cancer cell proliferation and migration in luminal B breast cancer subtype. Cell Death Dis 12:171

Ramstedt B, Slotte JP (2006) Sphingolipids and the formation of sterol-enriched ordered membrane domains. Biochim Biophys Acta 1758:1945–1956

Rani CSS, Abe A, Chang Y, Rosenzweig N, Saltiel AR, Radin NS, Shayman JA (1995) Cell cycle arrest induced by an inhibitor of glucosylceramide synthase. Correlation with cyclin-dependent kinases. J Biol Chem 270:2859–2867

Rao BD, Sarkar P, Chattopadhyay A (2021) Effect of tertiary amine local anesthetics on G protein-coupled receptor lateral diffusion and actin cytoskeletal reorganization. Biochim Biophys Acta 1863:183547

Riethmüller J, Riehle A, Grassmé H, Gulbins E (2006) Membrane rafts in host-pathogen interactions. Biochim Biophys Acta 1758:2139–2147

Róg T, Orłowski A, Llorente A, Skotland T, Sylvänne T, Kauhanen D, Ekroos K, Sandvig K, Vattulainen I (2016) Interdigitation of long-chain sphingomyelin induces coupling of membrane leaflets in a cholesterol dependent manner. Biochim Biophys Acta 1858:281–288

Rosenhouse-Dantsker A, Mehta D, Levitan I (2012) Regulation of ion channels by membrane lipids. Compr Physiol 2:31–68

Ryland LK, Fox TE, Liu X, Loughran TP, Kester M (2011) Dysregulation of sphingolipid metabolism in cancer. Cancer Biol Ther 11:138–149

Sabbadini RA, Danieli-Betto D, Betto R (1999) The role of sphingolipids in the control of skeletal muscle function: a review. Ital J Neurol Sci 20:423–430

Saddoughi SA, Song P, Ogretmen O (2008) Roles of bioactive sphingolipids in cancer biology and therapeutics. Subcell Biochem 49:413–440

Sarkar P, Rao BD, Chattopadhyay A (2020) Cell cycle dependent modulation of membrane dipole potential and neurotransmitter receptor activity: role of membrane cholesterol. ACS Chem Neurosci 11:2890–2899

Schafer KA (1998) The cell cycle: a review. Vet Pathol 35:461–478

Shaw J, Costa-Pinheiro P, Patterson L, Drews K, Spiegel S, Kester M (2018) Novel sphingolipid-based cancer therapeutics in the personalized medicine era. Adv Cancer Res 140:327–366

Simons K, Ikonen E (1997) Functional rafts in cell membranes. Nature 387:569–572

Simons K, Toomre D (2000) Lipid rafts and signal transduction. Nat Rev Mol Cell Biol 1:31–39

Simons K, van Meer G (1988) Lipid sorting in epithelial cells. Biochemistry 27:6197–6202

Singh P, Paila YD, Chattopadhyay A (2012) Role of glycosphingolipids in the function of human serotonin$_{1A}$ receptors. J Neurochem 123:716–724

Singh P, Saxena R, Srinivas G, Pande G, Chattopadhyay A (2013) Cholesterol biosynthesis and homeostasis in regulation of the cell cycle. PLoS ONE 8:e58833

Slotte JP (2016) The importance of hydrogen bonding in sphingomyelin's membrane interactions with co-lipids. Biochim Biophys Acta 1858:304–310

Slotte JP, Bierman EL (1988) Depletion of plasma-membrane sphingomyelin rapidly alters the distribution of cholesterol between plasma membranes and intracellular cholesterol pools in cultured fibroblasts. Biochem J 250:653–658

Slotte JP, Tenhunen J, Pörn I (1990) Effects of sphingomyelin degradation on cholesterol mobilization and efflux to high-density lipoproteins in cultured fibroblasts. Biochim Biophys Acta 1025:152–156

Smith PK, Krohn RI, Hermanson GT, Mallia AK, Gartner FH, Provenzano MD, Fujimoto EK, Goeke NM, Olson BJ, Klenk DC (1985) Measurement of protein using bicinchoninic acid. Anal Biochem 150:76–85

Sonnino S, Prinetti A (2016) The role of sphingolipids in neuronal plasticity of the brain. J Neurochem 137:485–488

Stockmann-Juvala H, Savolainen K (2008) A review of the toxic effects and mechanisms of action of fumonisin B_1. Hum Exp Toxicol 27:799–809

Taniguchi Y, Ohba T, Miyata H, Ohki K (2006) Rapid phase change of lipid microdomains in giant vesicles induced by conversion of sphingomyelin to ceramide. Biochim Biophys Acta 1758:145–153

van Echten-Deckert G, Walter J (2012) Sphingolipids: critical players in Alzheimer's disease. Prog Lipid Res 51:378–393

van Meer G, de Kroon AIPM (2011) Lipid map of the mammalian cell. J Cell Sci 124:5–8

van Meer G, Lisman Q (2002) Sphingolipid transport: rafts and translocators. J Biol Chem 277:25855–25858

Vistica DT, Skehan P, Scudiero D, Monks A, Pittman A, Boyd MR (1991) Tetrazolium-based assays for cellular viability: a critical examination of selected parameters affecting formazan production. Cancer Res 51:2515–2520

Viswanathan G, Jafurulla M, Kumar GA, Raghunand TR, Chattopadhyay A (2018) Macrophage sphingolipids are essential for the entry of *Mycobacteria*. Chem Phys Lipids 213:25–31

Voss KA, Riley RT (2013) Fumonisin toxicity and mechanism of action: overview and current perspectives. Food Safety 1:49–69

Wang E, Norred WP, Bacon CW, Riley RT, Merrill AH Jr (1991) Inhibition of sphingolipid biosynthesis by fumonisins. Implications for disease associated with *Fusarium moniliforme*. J Biol Chem 266:14486–14490

Wang S-K, Wang T-T, Huang G-L, Shi R-F, Yang L-G, Sun G-J (2014) Stimulation of the proliferation of human normal esophageal epithelial cells by fumonisin B_1 and its mechanism. Exp Ther Med 7:55–60

Warnock DE, Roberts C, Lutz MS, Blackburn WA, Young WW Jr, Baenziger JU (1993) Determination of plasma membrane lipid mass and composition in cultured Chinese Hamster Ovary cells using high gradient magnetic affinity chromatography. J Biol Chem 268:10145–10153

Zeidan YH, Hannun YA (2007) Translational aspects of sphingolipid metabolism. Trends Mol Med 13:327–336